High-pressure Brillouin scattering study on Ar hydrate

2002 J. Phys.: Condens. Matter 14 10679

(http://iopscience.iop.org/0953-8984/14/44/356)

INSTITUTE OF PHYSICS PUBLISHING JOURNAL OF PHYSICS: CONDENSED MATTER

J. Phys.: Condens. Matter **14** (2002) 10679–10682 PII: S0953-8984(02)39735-2

High-pressure Brillouin scattering study on Ar hydrate

I Suwa[1], **T Kato**[1], **S Sasaki**[1,2] **and H Shimizu**[1,2]

[1] Department of Electrical and Electronic Engineering, Gifu University, 1-1 Yanagido, Gifu 501-1193, Japan
[2] CREST, Japan Science and Technology Corporation, Saitama 332-0012, Japan

Received 1 June 2002
Published 25 October 2002
Online at stacks.iop.org/JPhysCM/14/10679

Abstract

The pressure dependence of the elastic properties of sII-type Ar hydrate has been determined up to 0.70 GPa at room temperature by using a high-pressure Brillouin scattering method. At about 0.10 GPa, ratios of the elastic constants to the density of $C_{11}/\rho = 10.16$, $C_{12}/\rho = 6.30$, $C_{44}/\rho = 2.32 \times 10^6$ m^2 s^{-2} are obtained. Comparing with sI-type CH_4 hydrate, the acoustic velocities for the longitudinal acoustic and transverse acoustic modes of Ar hydrate (sII) were found to be about 15 and 25% lower, respectively.

1. Introduction

Gas hydrates are ice-like crystalline solids consisting of a framework of hydrogen-bonded water (H_2O) molecules (the host lattice) that trap the guest molecules. At present, it is known that there are two cubic hydrate structures (sI, sII) and one hexagonal structure (sH); which structure is found depends on the size of the guest molecules. Structure I (sI) is composed of two S-cages (5^{12}) and six M-cages ($5^{12}6^2$) in the unit cell. Structure II (sII) consists of sixteen S-cages (5^{12}) and eight L-cages ($5^{12}6^4$) in the unit cell, where both cages form a diamond-type cubic structure. Finally, the unit cell of hexagonal structure H (sH) contains three S-cages (5^{12}), two M-cages ($4^3 5^6 6^3$) and one L-cage ($5^{12}6^8$). In the case of argon (Ar) hydrate, small-size Ar atoms primarily fill many S-cages to form sII hydrate [1].

Recently, the decomposition curve of Ar hydrate has been investigated, and it is suggested that three or more hydrate phases exist up to 3.0 GPa and 140 °C [2, 3]. No detailed hydrate structures except for the low-pressure sII phase have been reported yet. At room temperature, Ar hydrate is formed as cubic sII at about 0.1 GPa, and the phase transition to the above Ar hydrate phase occurs at about 0.7 GPa.

The purpose of this paper is to report the growth of a single crystal of Ar hydrate in a diamond anvil cell (DAC) under high pressure at room temperature, and determination of the elastic properties, such as the acoustic velocities and ratios of elastic constants to the density of Ar hydrate, by using high-pressure Brillouin spectroscopy. Furthermore, we examine the difference in sound velocity between sII-type Ar hydrate and sI-type CH_4 hydrate [4].

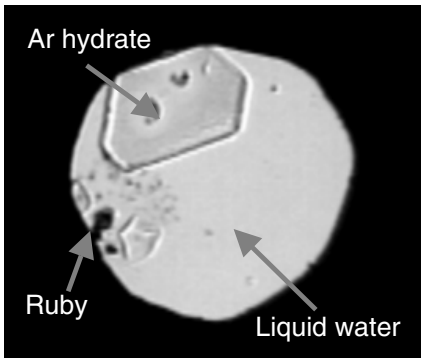

Figure 1. A photograph of a single crystal of Ar hydrate (sII) at $P = 0.17$ GPa. A small ruby chip is used for pressure calibration.

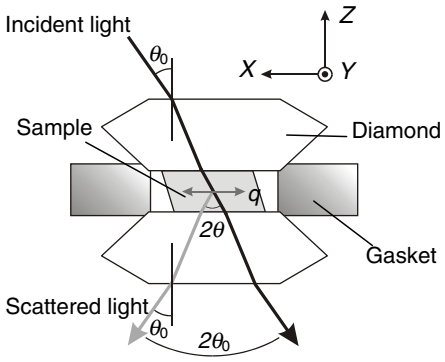

Figure 2. The scattering geometry in the DAC. For the 60° scattering geometry, the value of θ_0 is 30°. The wavevector of the acoustic phonon (q) is along the X-direction parallel to the diamond interfaces (XY-plane).

2. Experimental details

In order to seal both H_2O and Ar into the DAC, Ar gas was compressed above critical pressure and was loaded into a small chamber (400 μm in diameter, 40 μm in depth) of the DAC filled with pure water. At room temperature, the transition from liquid H_2O + liquid Ar to polycrystal Ar hydrate + liquid H_2O + liquid Ar occurs at about 0.10 GPa [2, 3, 5]. In this state of coexistence of the three phases, we grew a single crystal of Ar hydrate by controlling the pressure and temperature as shown in figure 1.

Brillouin spectra were measured in a 60° scattering geometry using a tandem Fabry–Perot interferometer (JRS). Since the single crystal of Ar hydrate is completely in contact with both upper and lower diamond interfaces, there is no disturbance of the scattering geometry by liquid H_2O (see figure 2). The 514.5 nm line of an argon-ion laser with single-frequency operation was used for excitation with an input power of below 40 mW.

Brillouin frequency shifts in the 60° scattering geometry ($\Delta\nu_{60}$) with the DAC ($\theta_0 = 30°$ in figure 2) are immediately transformed to acoustic velocities v_{60} by using the equation $v_{60} = \Delta\nu_{60}\,\lambda_0$, where λ_0 is the wavelength of the incident light. The observed wavevector of the acoustic phonon (q) is along the X-direction of the laboratory frame and is also parallel to the interfaces of the diamond anvils. By rotation of the DAC about the Z-axis, the acoustic phonons (q) propagating in any direction parallel to XY-plane can be observed.

In order to analyse the elastic waves as a function of rotation angle ϕ, it is necessary to use Every's expression relating the acoustic velocities for arbitrary directions to the elastic constants [6]. We can easily modify Every's expression for cubic crystals to one applicable to the present experimental system by using the Euler angles (θ, ϕ, χ) relating the laboratory frame (X, Y, Z) to the crystalline axis frame instead of the direction cosines of the phonon's wavevector. Consequently, the velocities for three acoustic modes can be expressed as a function of six parameters: $v_k = f_k(C_{11}/\rho, C_{12}/\rho, C_{44}/\rho, \theta, \phi, \chi)$, where the subscript k indicates the LA, TA_1 and TA_2 modes, the C_{ij} are three elastic constants for the cubic system, ρ is the density of the specimen and ϕ corresponds to the angle of rotation around the Z-axis. By applying the least-squares fitting method to the experimental data and the above theoretical velocities, three ratios of elastic constants to the density ($C_{11}/\rho, C_{12}/\rho, C_{44}/\rho$) and two Euler angles ($\theta, \chi$) are obtained simultaneously.

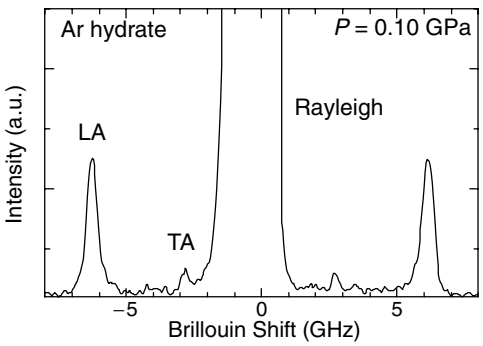

Figure 3. Typical Brillouin spectrum of Ar hydrate (sII) at about 0.10 GPa. LA and TA indicate the longitudinal and transverse acoustic modes, respectively.

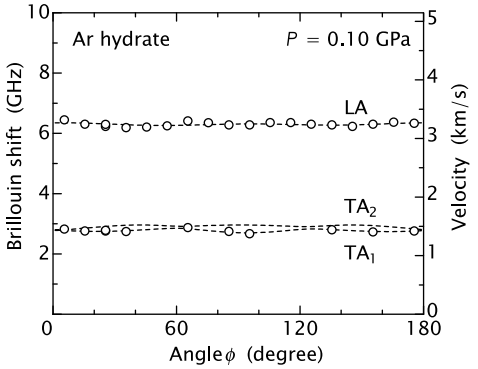

Figure 4. Brillouin frequency shifts (GHz) and sound velocities (km s^{-1}) of LA and TA modes of Ar hydrate (sII) as a function of angle ϕ at about 0.10 GPa. Open circles indicate the experimental points and the broken curves represent the best-fitted theoretical curves.

3. Results and discussion

By applying high-pressure Brillouin spectroscopy to a single crystal of Ar hydrate at about 0.10 GPa, we obtained a Brillouin spectrum as shown in figure 3. The longitudinal acoustic (LA) and transverse acoustic (TA) modes are observed. As for TA mode, two signals should be detected. However, the only one peak is observed because of its weak intensity and slight dependence on angle ϕ. To confirm whether the Brillouin spectrum obtained is originating from Ar hydrate, we measured the Brillouin spectrum of liquid H_2O around the Ar hydrate. As a result, only one LA mode was detected, at about Brillouin shift of 3.5 GHz. Therefore, the spectrum shown in figure 3 is certainly from Ar hydrate.

Figure 4 shows the acoustic velocities (Brillouin frequency shifts) as a function of ϕ at about 0.10 GPa. It is clear from figure 4 that both LA and TA modes are almost constant against ϕ, which means the Ar hydrate is nearly elastically isotropic. On the assumption that the elastic anisotropy of Ar hydrate is equal to 1 ($A = 2C_{44}/(C_{11} - C_{12}) = 1$), the LA and TA velocities correspond to $(C_{11}/\rho)^{1/2}$ and $(C_{44}/\rho)^{1/2} = [(C_{11} - C_{12})/(2\rho)]^{1/2}$, respectively. From figure 4, we obtained $v_{LA} = 3.24$ km s^{-1} and $v_{TA} = 1.43$ km s^{-1}. As a result, the ratios of the elastic constants to the density were calculated to be $C_{11}/\rho = 10.5$, $C_{12}/\rho = 6.44$ and $C_{44}/\rho = 2.03 \times 10^6$ m^2 s^{-2}. Next, to determine the C_{ij}/ρ by analysing the experimental data plotted as open circles, we used the least-squares fitting method. The best-fitted theoretical curves indicated by broken curves in figure 4 were obtained; they yield $C_{11}/\rho = 10.16$, $C_{12}/\rho = 6.30$, $C_{44}/\rho = 2.32 \times 10^6$ m^2 s^{-2}. From these values, the elastic anisotropy is calculated to be $A = 1.20$. The differences between the C_{ij}/ρ on the assumption $A = 1$ and those from the least-squares method are within 10%. For the present, we employed the results from the least-squares method, since the acoustic velocities of Ar hydrate have a slight dependence on angle ϕ as shown in figure 4. The pressure dependence of the C_{ij}/ρ for Ar hydrate up to 0.70 GPa are shown in figure 5. It is notable that the pressure dependence of C_{44}/ρ is almost constant in contrast to the positive pressure dependences of C_{11}/ρ and C_{12}/ρ, which means the Ar hydrate becomes weak against shear stress with increasing pressure.

Figure 6 shows the pressure dependences of the acoustic velocities for propagation along the ⟨100⟩ direction of Ar hydrate (sII) together with those of CH_4 hydrate (sI) for comparison. It is clear that the acoustic velocities for both LA and TA modes of Ar hydrate are lower than

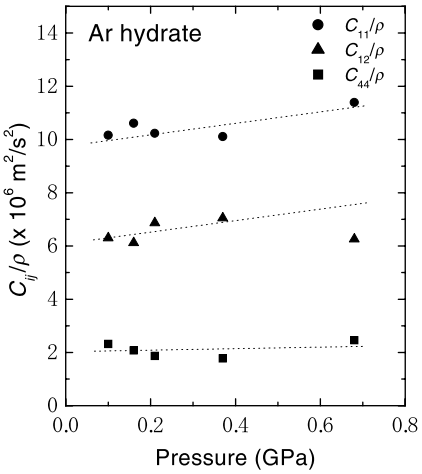

Figure 5. The pressure dependence of C_{ij}/ρ for Ar hydrate at room temperature.

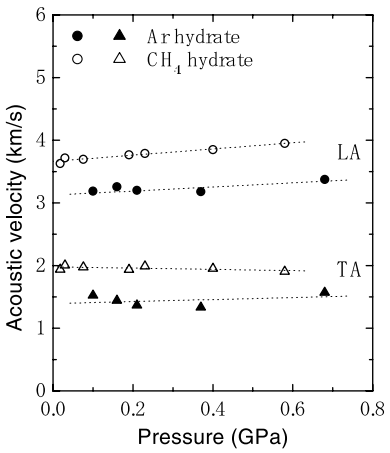

Figure 6. The pressure dependences of the acoustic velocities for propagation along the ⟨100⟩ direction at room temperature. Solid and open symbols are for Ar hydrate (sII) and CH_4 hydrate (sI).

those of CH_4 hydrate, respectively. This difference is basically caused by the density of Ar hydrate being higher than that of CH_4 hydrate. To obtain the intrinsic difference between the sI and sII hydrates, we calculate the ratios of acoustic velocities v_{TA}/v_{LA} to be about 0.45 for sII-type Ar hydrate and about 0.52 for sI-type CH_4 hydrate. This shows that the TA velocity of Ar hydrate is lower than that of CH_4 hydrate. In other words, sII-type hydrate is weaker against shear stress than sI-type hydrate.

4. Conclusions

The elastic properties of Ar hydrate have been determined as a function of pressure at room temperature. From these results, a single crystal of Ar hydrate of sII type is probably weak against shear stress. In order to estimate safe conditions for mining the natural hydrate from deep sea deposits, more detailed dynamical studies (e.g. decomposition experiments on hydrates using direct uniaxial and shear stress) and x-ray diffraction experiments will be needed.

Acknowledgment

This research was supported in part by an Iwatani Naoji Foundation research grant.

References

[1] Tanaka H 1995 *Fluid Phase Equilib.* **104** 331
[2] Dyadin Y A *et al* 1997 *Mendeleev Commun.* **1** 32
[3] Lotz H T and Schouten J A 1999 *J. Chem. Phys.* **111** 10 242
[4] Sasaki S *et al* 2002 *J. Phys.: Condens. Matter* **14**
[5] Marshall D R, Saito S and Kobayashi R 1964 *AIChE J.* **10** 202
[6] Every A G 1979 *Phys. Rev. Lett.* **42** 1065